A robust and fast sliding mode controller for position tracking control of permanent magnetic synchronous motor

Junfeng Jiang [1,2] and *Xiaojun* Zhou [1,2]

[1] State Key Laboratory of Fluid Power and Mechatronic Systems, Zhejiang University, Hangzhou, 310027, Zhejiang, China
[2] Zhejiang Province Key Laboratory of Advanced Manufacturing Technology, Zhejiang University, Hangzhou, 310027, Zhejiang, China

Abstract. The permanent magnet synchronous motor (PMSM) is important in position tracking applications. A performance degradation is caused by the internal uncertainties and external load disturbance. To achieve a high control performance, a fast and precise control scheme with great robustness has to be applied. In this paper, we propose a composite control method for PMSM systems by combing the extended state observer (ESO) technique with fast terminal sliding mode (FTSM) control. The FTSM guarantees the fast convergence rate and the ESO can estimate the disturbance accurately. The proposed method has a fast response and a good disturbance rejection property compared with other sliding mode methods. Simulations are carried out to show the effectiveness of this method.

1 Introduction

The permanent magnet synchronous motor (PMSM) is extensively employed in high-performance drive systems. This is mainly due to its compactness, high efficiency, and high torque-to-inertia ratio [1, 2]. It is well known that PMSM systems are confronted with external disturbance and internal parameter variations [3]. Therefore, it is unrealistic to obtain a satisfactory control performance only by linear control scheme such as proportional-integral controller. To enhance the control performance of PMSM systems, many nonlinear and advanced control schemes have been adopted [4], e.g., adaptive control [5], predictive control [6], intelligent control [7], sliding mode control (SMC) [8] and so on.

Among the aforementioned methods, the SMC has been successfully applied due to its invariant properties to internal uncertainties and external disturbances. In general, there are three steps to be considered to design a SMC scheme: the choice of a sliding mode surface, the design of a reaching law and the determination of a control law. The conventional SMC has a linear sliding surface with asymptotical stability. To achieve finite-time stabilization, terminal sliding mode (TSM) concept has been proposed [9]. It has been adopted in the control of rigid manipulators [10]. However, there are negative fractional powers in the TSM control law, which may arise the singularity problem. Non-singular TSM (NTSM) has been proposed to avoid singularity phenomenon. In addition, it maintains the advantages of traditional TSM such as finite time stability [11]. However, the reaching law of NTSM is discontinuous. Consequently, the undesirable chattering is caused. To eliminate the chattering effect, a continuous NTSM (CNTSM) with a continuous reaching law has been developed [12]. It can not only eliminate the chattering, but also stabilize the system in finite time. In addition, the control law of CNTSM is non-singular [13]. However, there are two problems hindering the use of CNTSM control as follows:

(1) The nonlinear sliding surface makes the convergence rate slow in comparison with the linear one. This phenomenon is caused especially when the system state is far away from the equilibrium.

(2) High gain is needed for CNTSM control when the PMSM system is affected by strong disturbance. Therefore, large steady-state fluctuations are caused. In addition, a prior knowledge of the bound of lumped disturbance is required to obtain enough robustness. It is impossible in real applications.

To enhance system performance in the presence of multiple disturbance, the extended state observer (ESO) technique has been developed [14, 15]. It regards the lumped disturbance as a new system state and can estimate both disturbance and states [16]. Therefore, a feedforward compensation can be introduced into the controller design.

In this paper, a fast terminal sliding mode (FTSM) control with continuous reaching law is applied in the position tracking control of PMSM systems. The sliding surface of FTSM has both linear and non-linear terms such that fast and finite-time convergence is achieved. Then, combining the FTSM control and the extended ESO technique, a robust FTSM (RFTSM) control method is developed for the tracking control of PMSM systems. The proposed method has a fast convergence rate compared with ordinary SMC such as TSM control, NTSM control and CNTSM control. In addition, it can

estimate the lumped disturbance accurately. Hence, a good robustness with respect to external disturbance and internal uncertainties is obtained. Comparative simulations are performed to validate the effectiveness of the proposed method.

2 Mathematical model of PMSM

Taking the rotor coordinates (*d-q* axis) of the motor as reference coordinates, the flux linkage equations of the PMSM can be expressed as

$$\psi_d = L_d i_d + \psi_r$$
$$\psi_q = L_q i_q \tag{1}$$

where ψ_d, ψ_q are the flux linkage of d axis and q axis, respectively; L_d, L_q are the d-axis and q-axis inductance, respectively; i_d, i_q are the d and q axis stator currents, respectively; ψ_r is the flux linkage established by permanent magnet. Applying Kirchhoff's voltage law, the PMSM voltage equations can be represented as

$$u_d = \frac{d\psi_d}{dt} - \omega_r \psi_q + R_s i_d$$
$$u_q = \frac{d\psi_q}{dt} + \omega_r \psi_d + R_s i_q \tag{2}$$

where u_d, u_q are the d and q axis stator voltages, respectively; ω_r is the electrical angular velocity of the rotor; R_s is the stator resistance. In general, the d-axis reference current i_d^* is set to 0 to eliminate the couplings between speed and current. Output current i_d usually satisfies $i_d = i_d^* = 0$ because of the regulation of current controller [17]. Then the electromagnetic torque of PMSM can be expressed as

$$T_e = k_t i_q \tag{3}$$

with k_t the torque constant. Considering the friction damping and the load torque, the motion equation of the PMSM can be obtained as

$$\frac{J}{p_n} \dot{\omega}_r = T_e - T_L - B\omega_r \tag{4}$$

with J the system moment of inertia, p_n the number of pole pairs, T_L the load torque and B the viscous friction coefficient. So taking the angular position and speed as the system state variables, the following state-space model can be obtained

$$\begin{cases} \dot{\theta}_r = \omega_r \\ \dot{\omega}_r = \frac{p_n k_t}{J} i_q - \frac{p_n T_L}{J} - \frac{B p_n}{J} \omega_r = a i_q^* + b(\omega_r) + d \end{cases} \tag{5}$$

where θ_r is the electrical angular position of the rotor, i_q^* is the q-axis reference current and is also the control input in this paper, $a = \dfrac{p_n K_t}{J}$ is the control input constant, $b(\omega_r) = -\dfrac{n_p B}{J} \omega_r$ is the smooth function of ω_r, $d = -\dfrac{n_p K_t}{J}(i_q^* - i_q) - \dfrac{n_p}{J} T_L$ is the system disturbance.

3 Controller design

Let θ_{ref} be the position reference and define the tracking error as $e = \theta_r - \theta_{ref}$. The sliding surface of CNTSM introduced in [12] can be described as

$$s = e + \beta \dot{e}^{p/q} = 0 \tag{6}$$

where $\beta > 0$ is a design constant, and both p and q are positive odd integers satisfying $q < p < 2q$. The reaching law is

$$\dot{s} = -k_1 s - k_2 s^{q_0/p_0} \tag{7}$$

where k_1 and k_2 are positive design constants, and both p_0 and q_0 are positive odd integers satisfying $p_0 > q_0$. Combing model (5), sliding surface (6) together with reaching law (7), the CNTSM control law for PMSM can be deduced as

$$i_q^* = -a^{-1}(b(\omega_r) + k_1 s + k_2 s^{q_0/p_0} - \ddot{\theta}_{ref}$$
$$+ \beta^{-1} \frac{q}{p} \dot{e}^{2-p/q} + d) \tag{8}$$

One can see that the control law is continuous and has no terms with negative fractional powers. Therefore, the chattering and singularity can be eliminated.

However, the following equation can be deduced according to (6)

$$\dot{e} = -\beta^{q/p} e^{q/p} \tag{9}$$

One can see that the absolute value of $\dot{e}$ is much smaller than that of linear sliding surface ($p=q$) when e is far away from zero. Therefore, the convergence rate of nonlinear sliding surface is slower. It should be noted that the result reverses when e is close to zero. The reason is that $\dot{e}$ remains almost a constant on the linear sliding surface while grows exponentially on the nonlinear one.

To accelerate the convergence rate, the following fast terminal sliding mode is applied [18]

$$s = \dot{e} + \alpha e + \beta e^{q/p} = 0 \tag{10}$$

where $\alpha > 0$ is a constant. When e is far away from zero, the derivative of tracking error can be approximately represented as $\dot{e} = -\alpha e$. When e is close to zero, it can be approximately expressed as $\dot{e} = -\beta e^{q/p}$. As a result, the fast convergence rate of e can be guaranteed. The following FTSM control law for PMSM can be derived

$$i_q^* = -a^{-1}(b(\omega_r) + k_1 s + k_2 s^{q_0/p_0} - \ddot{\theta}_{ref}$$
$$+ \beta \frac{q}{p} e^{q/p-1} \dot{e} + \alpha \dot{e} + d) \tag{11}$$

We can see from CNTSM control (8) and FTSM control (11) that there is a disturbance term d. In real applications, it cannot be measured directly and its bound is hard to obtain. Therefore, d is usually set to zero. Thus performance degradation is caused because the system disturbance cannot be suppressed effectively. To improve the disturbance rejection property of this system, an ESO technique is incorporated to estimate the lumped disturbance.

A second-order linear ESO for PMSM system (5) can be designed as follows [19]

$$\begin{cases} \dot{\hat{\omega}}_r = \hat{d} - 2p(\hat{\omega}_r - \omega_r) + ai_q^* \\ \dot{\hat{d}} = -p^2(\hat{\omega}_r - \omega_r) \end{cases} \quad (12)$$

where $\hat{\omega}_r$ and $\hat{d}$ are the estimate of ω_r and d, respectively, and $-p$ is the desired double pole of the ESO with $-p < 0$. Thus, the RFTSM control method for PMSM can be expressed as

$$i_q^* = -a^{-1}(b(\omega_r) + k_1 s + k_2 s^{q_0/p_0} - \ddot{\theta}_{ref}$$
$$+ \beta \frac{q}{p} e^{q/p-1} \dot{e} + \alpha \dot{e} + \hat{d}) \quad (13)$$

Compared with control law (8) and (11), control law (13) has a disturbance compensation term $\hat{d}$. Therefore, it has a better disturbance rejection property.

4 Simulation results and discussion

To demonstrate the effectiveness of the proposed RFTSM method, comparative simulations have been performed in MATLAB/Simulink R2017a. Three methods, i.e., CNTSM, FTSM and RFTSM are applied for position tracking of PMSM systems. The position reference is $\theta_{ref} = 60\cos(\pi/2t)$ deg and the control input saturation is ± 30 A. External load torque $T_L = 30$ Nm is added from $t = 0.5$ s to $t = 0.6$ s. In the two current loops, the proportional gain $K_p = 150$ and the integral gain $K_i = 750$. Table 1 shows parameters of the PMSM used in this paper.

Table 1. Parameters of the PMSM.

Parameters	Values
Rated power	1.5 KW
Rated torque	14.32 Nm
Rated speed	1000 rpm
Stator resistance	1.79 Ω
Pole pairs	4
Torque constant	2.45 Nm/A
System moment of inertia	1.792×10^{-3} kg.m2
Viscous friction coefficient	9.403×10^{-5} Nm.s/rad
Stator inductance	6.68×10^{-3} H
Flux linkage	0.4083 Wb

4.1 Simulation results

The parameters of CNTSM are: $k_1 = 150$, $k_2 = 150$, $q_0 = 1$, $p_0 = 5$, $p = 5$, $q = 1$, $\beta_2 = 1/260$. One can see from Fig. **1** that the position response converges to the reference in finite time and tracks it well. However, the convergence rate is slow as shown in Fig. **1**(b). Besides, The steady state error is large because of the impact of the lumped disturbance. In addition, there are obvious fluctuations when the external disturbance is added or removed.
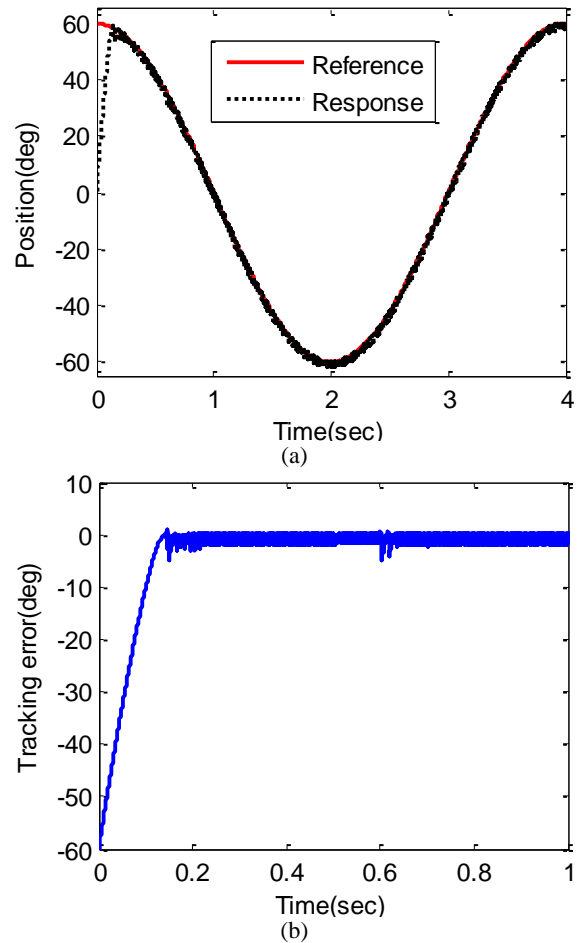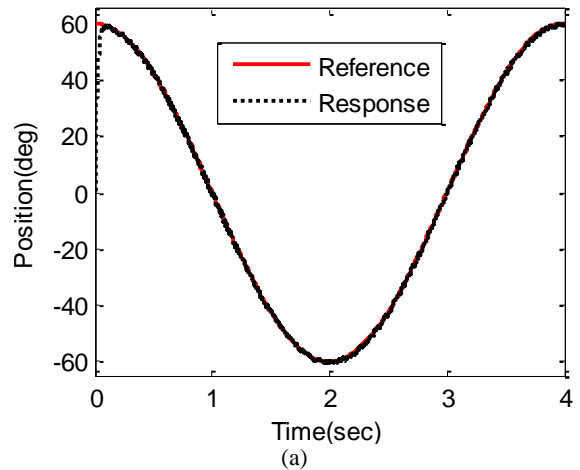

Fig. 1. Results of CNTSM. (a) Position reference and response, (b) tracking error.

The parameters of FTSM are selected as: $\alpha = 150$, $\beta = 150$, $p = 7$, $q = 1$, $p_0 = 9$, $q_0 = 1$, $k_1 = 70$, $k_2 = 30$. The simulation results of FTSM are shown in Fig. **2**. It is obvious that the convergence time of FTSM is much shorter than that of CNTSM. In addition, the steady tracking error and disturbance fluctuation are smaller. However, the tracking error is still a little large and the fluctuations still exist due to external disturbance.
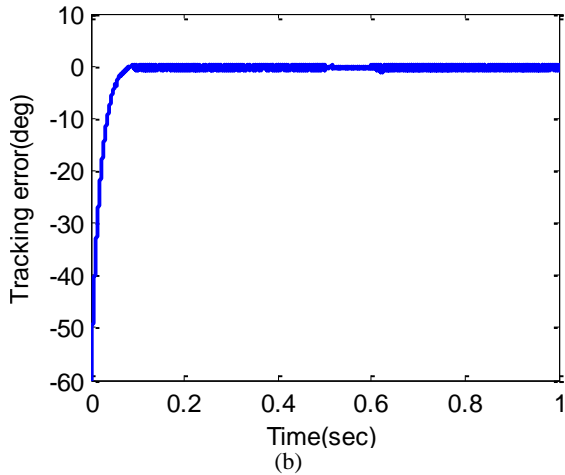
Fig. 2. Results of FTSM. (a) Position reference and response, (b) tracking error.
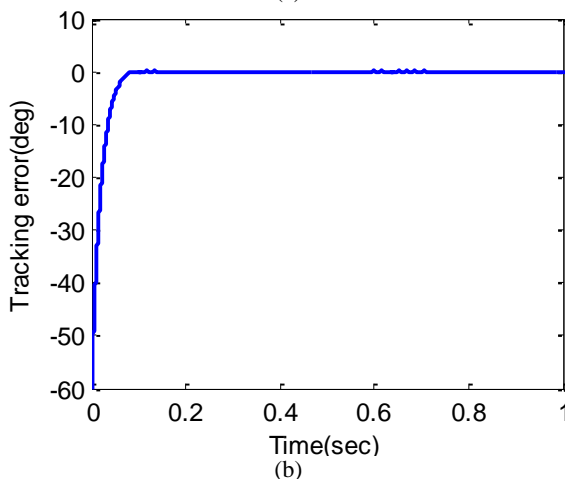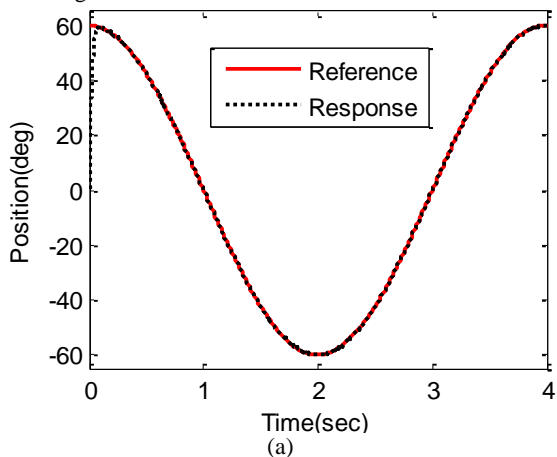

Fig. 3. Results of RFTSM. (a) Position reference and response, (b) tracking error.

For RFTSM, the pole of ESO is $-p=-50000$ and the other parameters are the same as those of FTSM. The simulation results are shown in Fig. **3**. We can see that a fast, high-precision and robust performance is achieved. The response converges to the reference fast and the tracking error is negligible. Moreover, the impact of the external disturbance is eliminated. The reason can be found in Fig. **4**. It is evident that the ESO can estimate the disturbance accurately. Hence, the system disturbance can be compensated by subtracting the estimated disturbance from the control input.

Fig. **5** shows the tracking error under RFTSM control method with perturbation in system inertia. The tracking errors of different system inertias is summarized in Table 2. $J_0=1.792 \times 10^{-3}$ kg.m^2 is the initial value of system inertia. One can see that the tracking error tends to be larger with the increase of system inertia. However, it remains small in all cases and the control performance remains satisfactory. Thus, we can conclude that the proposed RFTSM method has a strong robustness with respect to external disturbance and internal uncertainties.
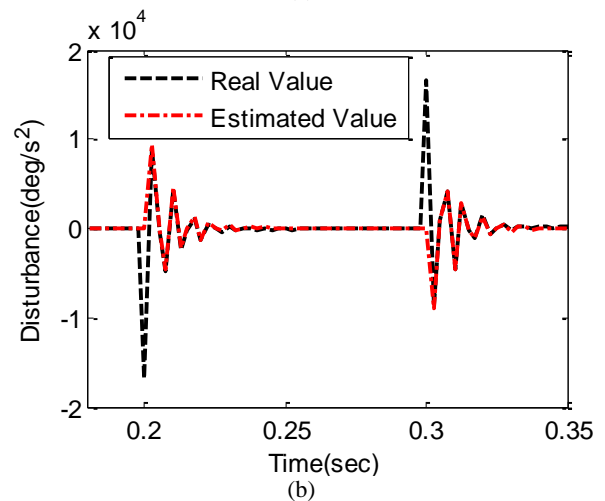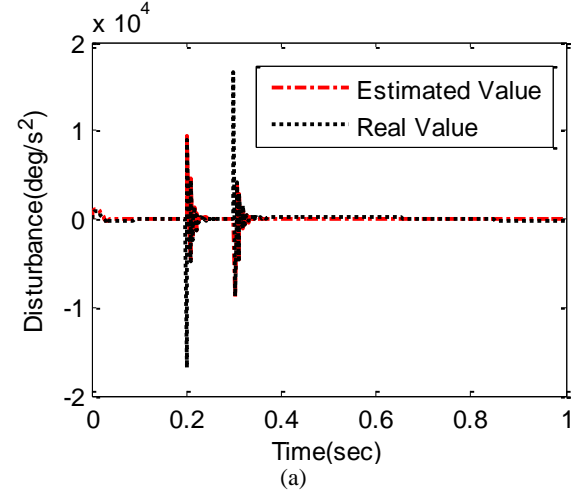

Fig. 4. Estimated disturbance values of ESO and real disturbance values. (a) Original figure, (b) zoomed figure.
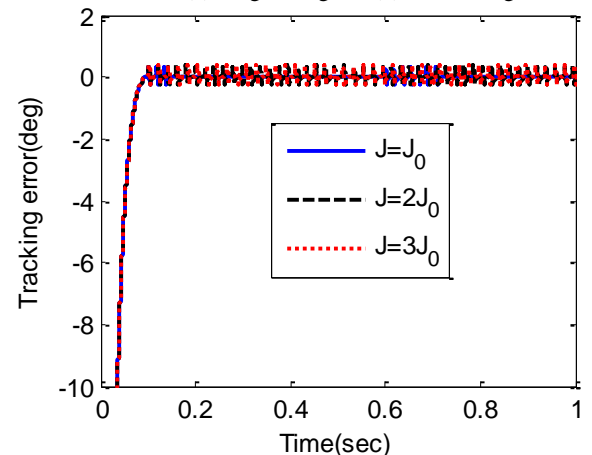

Fig. 5. Tracking error under RFTSM with perturbations in system inertia.

Table 2. Tracking errors with perturbation in system inertia

Values of system inertia	Steady tracking error (deg)
$J=J_0$	0.01
$J=2J_0$	0.38
$J=3J_0$	0.40

4.2 Discussion

To make clear comparisons, the simulation tracking performances of three methods are summarized in Table 3. It can be observed that the settling time of RFTSM is reduced by 46.7% compared with the CNTSM method. The steady tracking error is reduced by 99.5% and 98.6% compared with CNTSM and FTSM, respectively. In addition, the disturbance fluctuation under the proposed RFTSM method has reduced to a negligible magnitude.

It should be noted that there is a term $\beta \frac{q}{p} e^{q/p-1} \dot{e}$ with a negative fractional power in expression (11) and (13). This means singularity problem may appear under FTSM or RFTSM control method. However, this problem can be easily overcome by the saturation function of controllers.

Table 3. Tracking performance comparisons of three control schemes

Control schemes	Settling time (s)	Steady tracking error (deg)	Maximum disturbance fluctuation (deg)
CNTSM	0.15	2.09	4.76
FTSM	0.08	0.74	1.1
RFTSM	0.08	0.01	0.34

5 Conclusion

A fast and robust sliding mode control scheme is proposed for position tracking control of PMSM systems. This paper makes two contributions. First, the FTSM control method is applied such that the system state θ_r converges to the position reference θ_{ref} fast. Second, the ESO technique has been incorporated into FTSM method to enhance the disturbance rejection capacity of PMSM systems. Comparative simulations have been carried out to validate the effectiveness of the proposed method. Simulation results show that the proposed RFTSM method has a fast and precise performance in position tracking control. In addition, a strong robustness against internal uncertainties and external disturbance is achieved.

This method can also be applied in positioning control and speed regulation control of PMSM servo systems.

References

1. O. Saadaoui, A. Khlaief, M. Abassi, A. ChaariM. Boussak, IJC. **90**, 377–392 (2017).
2. A.R.I. Mohamed, ITIE. **54**, 1981–1988 (2007).
3. S. Li, H. Sun, J. Yang, X. Yu, ITAC. **60**, 277–282 (2015).
4. X. Zhang, L. Sun, K. Zhao, L. Sun, ITPE. **28**, 1358–1365 (2013).
5. H.H. Choi, N.T.T. Vu, J.W. Jung, ITPE. **26**, 3–8 (2011).
6. D. Zhi, L. Xu, B.W. Williams, ITPE. **25**, 341–351 (2010).
7. M. Singh, A. Chandra, ITPE. **26**, 165–175 (2011).
8. J. Yang, S. Li, J. Su, X. Yu, Autom. **49**, 2287–2291 (2013).
9. Z. Man, A.P. Paplinski, H.R. Wu, ITAC. **39**, 2464–2469 (1994).
10. Y. Tang, Autom. **34**, 51–56 (1998).
11. Y. Feng, X. Yu, Z. Man, Autom. **38**, 2159–2167 (2002).
12. S. Yu, X. Yu, B. Shirinzadeh, Z. Man, Autom. **41**, 1957–1964 (2005).
13. H. Wang, S. Li, Q. Lan, Z. Zhao, X. Zhou, T. I. MEAS. CONTROL **39**, 1195–1204 (2016).
14. M. Chen, P. Shi, C.C. Lim, ITAC. **60**, 3281–3286 (2015).
15. J. Han, ITIE. **56**, 900–906 (2009).
16. Y.X. Su, C.H. Zheng, B.Y. Duan, ITIE. **52**, 814–823 (2005).
17. S. Li, Z. Liu, ITIE. **56**, 3050–3059 (2009).
18. X. Yu, Z. Man, IEEE T. CIRCUITS-I. **49**, 261–264 (2002).
19. R. Miklosovic, Z. Gao, *Industry Applications Conference, 2004*. (2004).